Cellular and Molecular Bioengineering, Vol. 8, No. 1, March 2015 *(© 2015)* pp. 32–50
DOI: 10.1007/s12195-015-0377-8

Substrate Stiffness Affects Human Keratinocyte Colony Formation

HODA ZARKOOB,[1] SANDEEP BODDULURI,[1] SAILAHARI V. PONNALURI,[1] JOHN C. SELBY,[2] and EDWARD A. SANDER[1]

[1]Department of Biomedical Engineering, The University of Iowa, 1418 Seamans Center, Iowa City, IA 52242, USA; and [2]Department of Dermatology, Carver College of Medicine, The University of Iowa, 200 Hawkins Drive, Iowa City, IA 52242, USA

(Received 1 September 2014; accepted 12 January 2015; published online 24 January 2015)

Associate Editor Roger D. Kamm oversaw the review of this article.

Abstract—Restoration of epidermal organization and function in response to a variety of pathophysiological insults is critically dependent on coordinated keratinocyte migration, proliferation, and stratification during the process of wound healing. These processes are mediated by the reconfiguration of both cell–cell (desmosomes, adherens junctions) and cell–matrix (focal adhesions, hemidesmosomes) junctions and the cytoskeletal filament networks that they serve to interconnect. In this study, we investigated the role of substrate elasticity (stiffness) on keratinocyte colony formation *in vitro* during the process of nascent epithelial sheet formation as triggered by the *calcium switch* model of keratinocyte culture. Keratinocytes cultured on pepsin digested type I collagen coated *soft* (nominal E = 1.2 kPa) polyacrylamide gels embedded with fluorescent microspheres exhibited (i) smaller spread contact areas, (ii) increased migration velocities, and (iii) increased rates of colony formation with more cells per colony than did keratinocytes cultured on *stiff* (nominal E = 24 kPa) polyacrylamide gels. As assessed by tracking of embedded microsphere displacements, keratinocytes cultured on *soft* substrates generated large local substrate deformations that appeared to recruit adjacent keratinocytes into joining an evolving colony. Together with the observed differences in keratinocyte kinematics and substrate deformations, we developed two *ad hoc* analyses, termed distance rank and radius of cooperativity, that help to objectively ascribe what we perceive as increasingly *cooperative* behavior of keratinocytes cultured on *soft* vs. *stiff* gels during the process of colony formation. We hypothesize that the differences in keratinocyte colony formation observed in our experiments could be due to cell–cell mechanical signaling generated *via* local substrate deformations that appear to be correlated with the increased expression of β4 integrin within keratinocytes positioned along the periphery of an evolving cell colony.

Keywords—Epithelial sheet, Traction microscopy, Polyacrylamide, Mechanosensing.

Address correspondence to John C. Selby, Department of Dermatology, Carver College of Medicine, The University of Iowa, 200 Hawkins Drive, Iowa City, IA 52242, USA; Edward A. Sander, Department of Biomedical Engineering, The University of Iowa, 1418 Seamans Center, Iowa City, IA 52242, USA. Electronic mails: john-selby@uiowa.edu, edward-sander@uiowa.edu

INTRODUCTION

The human epidermis, composed of its principal cell type, the keratinocyte, plays an important role in the barrier function of skin, essential to the physiologic processes of water homeostasis, photoprotection from UV-induced damage, and immune surveillance.[31] Central to its biomechanical function, the epidermis is endowed with the ability to regenerate following a variety of different pathophysiological insults. Keratinocyte migration, proliferation, and stratification during the process of wound healing represent the body's attempt to restore the complex organization and function of the tissue.[9,22] This organization is critically dependent on the arrangement of interconnecting desmosomes, adherens junctions, focal adhesions, hemidesmosomes, and transcellular intermediate filament networks. These and other cytoskeletal proteins are responsible for the biomechanical properties of the epidermis. Coupled with fibroblast-mediated repair and reorganization of the dermal extracellular matrix (ECM), investigations focused on enhancing our understanding of the mechanobiological process of wound healing represent an important and ongoing topic of active research.

Under normal physiologic conditions *in vivo*, keratinocytes at the wound margins must form cell–matrix adhesions in order to migrate, proliferate, and reform a continuous epithelial barrier spanning the zone of damaged tissue. The ECM that keratinocytes are in contact with throughout this process—clinically referred to as *granulation tissue*—is dynamic in both composition and structure. By necessity, the ability of keratinocytes to sense and respond to changes in such a dynamic mechanical environment must play an integral role in the process of wound healing and the structure–function relationships that develop within the epidermis post-tissue repair.[10] Past works have

shown that keratinocyte force generation, morphology, migration, and differentiation *in vitro* can be modulated *via* changes in the elasticity (or stiffness) of the culture substrate, geometric constraints on cell shape and spreading, the physical dimensionality of the culture system (2D vs. 3D), and the biochemical specificity of ECM proteins available for the formation of adhesive contacts.[8,23,35,38,40]

More recently, researchers have explored the mechanobiology of monolayer epithelial sheets *via* traction force microscopy (TFM) experiments that probe the migratory behaviors of Madin–Darby canine kidney epithelial cells during the attempted closure of geometrically prescribed defects both internal and external to the boundaries of the monolayer.[2,17,36] As a fiducial model of epithelial sheet mechanics, these studies provide novel insight into the potential behavior of keratinocytes within the context of wound healing. Collectively, however, these studies are focused on the movements of a monolayer epithelial sheet, and not the behaviors of individual cells during the initial formation of the sheet. Although not universally recognized as a mechanism of re-epithelialization, it is conceivable that *individual* keratinocyte migration, proliferation, and colony formation may play a role in the re-epithelialization of large wounds *in vivo*. Moreover, individual keratinocyte migration, proliferation, and colony formation may also represent the primary mechanism by which liquid spray-applied keratinocyte cell-based therapies contribute to the enhanced re-epithelialization of chronic human venous ulcers observed in some clinical trials.[16,18] Arguably, experiments that assay the migration, proliferation, and differentiation of *individual* keratinocytes during the process of re-epithelialization will not only increase our understanding of the physiology of wound healing, but they will also aid in the development and optimization of cell-based wound care therapies of the future.

Towards this end, the purpose of this study was to investigate the role of substrate elasticity (stiffness) on keratinocyte colony formation *in vitro* during the process of nascent epithelial sheet formation as triggered by the *calcium switch* model of keratinocyte culture.[21,39,43] In this culture model, normal epidermal keratinocytes maintained in a proliferative monolayer state under low calcium concentrations (0.05–0.1 mM) are induced to form stable cell–cell junctions and stratify by increasing the calcium concentration of the culture media (1.2–1.8 mM). Using a combination of time-lapse differential interference contrast (DIC) microscopy and substrate displacement tracking microscopy, we monitored cell migration characteristics, rates of colony formation, cytoskeleton/cell morphology, and cell-generated substrate deformations for keratinocytes cultured on both *soft* (nominal 1.2 kPa) and *stiff* (nominal 24 kPa) polyacrylamide (PA) gels coated with covalently attached pepsin digested type I collagen and embedded with fluorescent microspheres, before, during, and after a *calcium switch*. In these experiments, keratinocytes cultured on *soft* PA gels migrated at increased velocities, produced substantially larger substrate displacements, and colonized faster *via* more cooperative cellular behaviors than did keratinocytes cultured on *stiff* PA gels. We hypothesize that the differences in colony formation observed in these experiments could be due to cell–cell mechanical signaling generated *via* local substrate deformations that appear to correlate with the increased expression of $\beta 4$ integrin within keratinocytes positioned along the periphery of the evolving cell colony.

MATERIALS AND METHODS

Cell Culture

Neonatal human epidermal keratinocytes (HEKn) (Invitrogen, Carlsbad, CA) were cultured in keratinocyte serum free medium (KSFM) (Invitrogen) supplemented with 1% penicillin–streptomycin and 0.1% amphotericin-B in a humidified incubator maintained at 37 °C and 95/5% air/CO_2. The baseline concentration of calcium in this supplemented medium is 0.09 mM, designated here as *Low* Ca^{2+} medium. *High* Ca^{2+} medium, with a calcium concentration of 1.2 mM, was created by adding $CaCl_2$ to KSFM medium supplemented with penicillin–streptomycin and amphotericin-B as noted above. HEKn were initially plated and passaged in *Low* Ca^{2+} medium using standard tissue culture polystyrene flasks. Passage 3 keratinocytes were used for all experiments.

Polyacrylamide Gels

The polyacrylamide (PA) gels used in these experiments were prepared using a modified version of the protocol described by Pelham and Wang.[25] Briefly, glass coverslips (40-mm circular No. 1½, Warner Instruments, Hamden, CT, and 12-mm circular No. 1, Fisher brand, Fischer Scientific, Pittsburgh, PA) were cleaned and etched with a 50:50 hydrochloric acid and methanol solution.[7] 40 mm coverslips were used for time-lapse imaging experiments and 12 mm coverslips were used for immunofluorescence studies. After washing, coverslips were *activated* with 0.1 N sodium hydroxide (Fisher Scientific), 100% 3-aminopropyltrimethyoxysilane (Sigma-Aldrich, St. Louis, MO), and 0.5% glutaraldehyde (Fisher Scientific). To fabricate either a *soft* or *stiff* PA gel, respectively, we combined 250 and 625 or 940 and 750 μL of

acrylamide and bis-acrylamide using stock solutions of acrylamide monomer (40% w/v, Bio-Rad, Hercules, CA) and bis-acrylamide (2% w/v, Fisher Scientific) that had been passed through a 0.2 μm filter. In a separate mixture, we added 100 μL of 0.5 μm diameter fluorescent microspheres (FluoSpheres® Ex/Em 580/605 nm, Life Technologies, Grand Island, NY), to either 3992.5 μL (*soft* gels) or 3180 μL (*stiff* gels) of deionized water, sonicating each solution for 15 min. The microsphere solutions were then added to their respective *soft* or *stiff* acrylamide/bis-acrylamide mixtures. Using a vortex mixer, we then added 7.5 μL of *N*,*N*,*N*′,*N*′ tetramethylethylenediamine (TEMED) (Fisher Scientific) to each acrylamide/bis-acrylamide/microsphere solution, immediately followed by a 15 min vacuum degas. Finally, 25 μL of 10% ammonium persulfate (APS) (Fisher Scientific) was added to each acrylamide/bis-acrylamide/microsphere/TEMED solution in order to initiate polymerization. For our time-lapse imaging experiments, 20 μL of either fully combined acrylamide/bis-acrylamide/microsphere/TEMED/APS solution was pipetted onto the surface of an *inactivated* Rain-X (ITW Global Brands, Houston, TX) treated glass microscope slide cut to measure 15 mm × 15 mm. An *activated* 40 mm cover glass slip was then placed on top of the liquid bead, in effect forming a thin liquid film between the microscope slide and cover glass. Our immunofluorescence specimens were prepared in a similar fashion, using 10 μL of either fully combined acrylamide/bis-acrylamide/microsphere/TEMED/APS solution, an uncut but *inactivated* Rain-X treated glass microscope slide, and *activated* 12 mm coverslips. After allowing the samples to polymerize for 15 min at room temperature, the Rain-X treated coverslips were removed. The resultant time-lapse and immunofluorescence specimens consisted of approximately 60–100 μm thick PA gels incorporated with fluorescent microspheres predominantly localized to the free surface of the gel. Upon completion of this initial fabrication sequence, all PA gel specimens were washed with phosphate buffered saline (PBS) and placed in sterile deionized water overnight on an orbital shaker to remove any unreacted residual acrylamide and bis-acrylamide.

In order to facilitate keratinocyte attachment for our calcium switch experiments, pepsin digested type I collagen was covalently attached to the surface of both *soft* and *stiff* PA gels using a protocol modified from Pelham and Wang.[25] Briefly, sulfosuccinimidyl 6(4-azido-2-nitrophenyl-amino) hexanoate (sulfo-SANPAH) (Thermo Scientific, Waltham, MA) was dissolved in DMSO (0.25 w/v) and then diluted in 50 mM 4-(2-hydroxyethyl)-1-piperazineethanesulfonic acid (HEPES) (adjusted to pH 8.5) to a final concentration of 0.2% v/v. The solution was added to the surface of each PA gel and placed under a UV light (Lamp XX-20BLB; 365 nm, 115 V, 20 W, Fisher Scientific) for 5 min. Samples were then washed with HEPES and a fresh mixture of sulfo-SANPAH and HEPES was added to the gel surface. Samples were then exposed to UV light for an additional 5 min. After a final HEPES wash, 100 μg/mL of pepsin digested type 1 collagen (PureCol® Advanced Biomatrix, San Diego, CA) was added to the surface of each PA gel and allowed to incubate at room temperature for 2 h. Unbound collagen was removed by rinsing the gels with PBS. PA gel substrates were sterilized under UV light (254 nm) in the biosafety cabinet for 15 min prior to initiating cell culture. Though not directly measured, the nominal moduli for the *soft* and *stiff* PA gels used in this work were assumed to be 1.2 and 24 kPa, respectively, as our gel formulations were nearly identical to those measured previously.[3,5]

Time-Lapse Live Cell Imaging

Time-lapse live cell images were acquired with a Nikon Eclipse Ti inverted microscope equipped with a perfect focus system, wide-field epifluorescence and DIC microscopy capabilities, a DS-Qi1 Nikon CCD camera, and a ProScan II motorized stage, all driven by NIS Elements software. DIC images for our cell tracking, counting, and classification analyses were obtained with a CFI Plan Apo 10× DIC objective (NA = 0.45), as were the fluorescent images used in our substrate deformation tracking analysis (cf. "Substrate Displacement Tracking" section). Inside the biosafety cabinet, a PA gel was placed in a temperature-controlled perfusion chamber (RC-31A, Warner Instruments). The keratinocytes were then plated onto the gel at a density of 4000 cells/cm^2 in *Low* Ca^{2+} medium (cf. "Cell Culture" section). Within 15 min, the chamber was mounted onto the microscope stage, the temperature was stabilized at 37 °C, and time-lapse imaging was initiated. Keratinocytes were allowed to attach and reach a relative equilibrium for 3 h before the calcium concentration of the medium was increased from *Low* Ca^{2+} to *High* Ca^{2+} *via* a syringe pump attached to the chamber. *High* Ca^{2+} medium was introduced to the chamber at a rate of 0.02 mL/min. The moment that the syringe pump was activated was designated as $t = 0$. The syringe pump was turned off at $t = 50$ min to ensure that at least two volume changes of the medium had occurred within the chamber. Time-lapse images were collected for a total of 24 h, after which, the experiment was terminated *via* introduction of trypsin to the perfusion chamber. For each discrete observation time, t, DIC and fluorescent (Ex/Em 545/620 nm) image pairs were acquired at four overlapping visual fields on the PA

gel. Of these four fields, the field with a keratinocyte count closest to 30 cells at time $t = 0$ was selected for use in the data analyses detailed in "Cell Classification and Counting, Cell Tracking, and "Substrate Displacement Tracking" sections. The time interval between images in our experiments was set at two minutes as a compromise between the need to minimize the keratinocytes' exposure to light (i.e., phototoxicity) and the need to minimize microsphere displacement tracking errors arising from large microsphere movements between subsequent image pairs. To ensure repeatability, three replicate experiments were performed on each type of PA gel substrate ($n = 3$ *soft* gels, $n = 3$ *stiff* gels). In addition, in order to provide some context for keratinocyte behavior in the absence of *High* Ca^{2+} medium, the experiment was repeated once on each substrate ($n = 1$ *soft* gel, $n = 1$ *stiff* gel) with exactly the same conditions except that *Low* Ca^{2+} medium was perfused through the chamber (starting at $t = 0$) instead of *High* Ca^{2+} medium.

Cell Classification and Counting

In order to differentiate between single cell and collective cell behaviors, keratinocytes observed in each acquired DIC image were classified as belonging to one of three groups: (i) *single cells*-individual keratinocytes lacking definitive cellular contacts along the entire periphery of its cell membrane; (ii) *cell couples*-two juxtaposed keratinocytes with a definitive area of mechanical contact formed by the apposition of their respective cell membranes; and (iii) *colonies*-three or more juxtaposed keratinocytes with multiple definitive areas of contact formed by the apposition of their respective cell membranes. In this classification scheme, cell couples were distinguished from colonies due to the possibility that cell couples could represent either a dividing cell or a transient cell–cell contact. The number of single cells, cell couples, and colonies were counted at every hour of the experiment. Regardless of their would-be classification, keratinocytes intersecting the border of each DIC image were excluded from the counts due to the uncertain presence of cell–cell contacts outside the field of view.

Cell Tracking

Cell migration was hand-tracked using the Manual Tracking plugin for ImageJ (National Institutes of Health, Bethesda, MD). The migratory path of a single keratinocyte i at time t in a DIC image was determined by clicking on the center of the cell nucleus and following it frame-by-frame until the cell reached the border of the field of view or until the keratinocyte joined a cell pair or colony. In this manner, an array of position vectors, $\vec{p}_i$, was created for the tracked keratinocyte. The process was repeated for all individual keratinocytes observed within the DIC image field. Although the time-lapse between DIC images was constant across all of our experiments, the total number of image frames counted for a given keratinocyte varied greatly, i.e., we could not control whether or not the keratinocyte being tracked remained within the field of view, nor could we control how quickly or slowly a keratinocyte being tracked joined a cell pair or colony.

Several parameters associated with keratinocyte migration and colony formation were calculated from the hand-tracked position vectors. First, the average instantaneous speed, $\langle S \rangle_i$, of cell i was calculated as $\langle s \rangle_i = {}^1/_N \sum_{t=1}^{N} |\vec{v}_i(t)|$, where N is total number of image frames counted for the keratinocyte being tracked, and $\vec{v}_i$ is the instantaneous velocity vector for cell i, calculated as $\vec{v}_i(t) = (\vec{p}_i(t) - \vec{p}_i(t - \Delta t))/\Delta t$, where Δt is the time-lapse interval between frames. A small number of cells (approximately 5–10% per frame) that left the image within the first 15 frames (i.e., 30 min) of the experiment were excluded from analysis in order to negate any effect the shear stress generated by the active flow of *High* Ca^{2+} medium into the perfusion chamber may have imposed on the initial migratory behaviors of the keratinocytes.

Second, an *ad hoc* ordinal distance rank (DR) was calculated for each single keratinocyte present in the field at time $t = 0$. To calculate this metric, we started with a single keratinocyte of interest at $t = 0$ and ranked the remaining keratinocytes in the visual field by order of the magnitude of their respective internuclear separation distances with the cell closest to the keratinocyte of interest being labeled with a rank of 1. All keratinocytes present within the field were rank ordered, regardless of whether or not they were present as single cells, couples, or colonies. Tracking keratinocytes forward in time, we then identified the rank of the cell that ultimately joined the original keratinocyte of interest to form a couple or colony. The ranking and tracking process was repeated for each single keratinocyte present within the DIC image at time $t = 0$.

Third, an *ad hoc* analysis we term the radius of cooperativity (RC) was calculated for each keratinocyte couple or colony present in our DIC images. To calculate this metric, we constructed a circle of radius, RC, centered on a keratinocyte couple or colony observed within the visual field. We then counted all cellular entities (single cells, couples, or colonies) that migrated into the circle, including entities in contact with only the peripheral margin of the circle. Tracking

these entities forward in time, we then calculated the percentage of entities initially localized to within the circle that ultimately joined the colony or couple under analysis. The calculations were repeated for each colony or couple formed within the DIC image during the course of the experiment.

Substrate Displacement Tracking

Substrate displacements generated by keratinocyte tractions on PA gels were measured by tracking the displacements of fluorescent microspheres embedded in our PA gels using a modified version of a template matching digital image correlation algorithm[27] applied to the fluorescent images collected during live time-lapse cell imaging. The algorithm, which uses normalized cross-correlation with an optimized sub-pixel displacement algorithm and local neighborhood smoothing, was applied to subsequent pairs of fluorescent microsphere images associated with times t and $t-\Delta t$. Embedded microsphere positions noted at the initialization of the experiment, i.e., just after cell seeding but prior to cell attachment, were used as the reference, or undeformed configuration of the gel. Note that in this version of the algorithm, the sub-pixel displacements were calculated using the algorithm proposed by Chan and Nguyen.[6] All displacement tracking and visualization was done in MATLAB (Mathworks, Natick, MA). In adjunctive studies to our major time-lapse cell imaging experiments, we attempted to perform simultaneous cell tracking and counting analyses and substrate displacement tracking using a CFI Plan-Apo 20× DIC objective (NA = 0.75) combined with a 1.5× magnifier. Although the higher magnification proved useful for resolving small substrate displacements on *stiff* gels (cf. "Substrate Displacements During Colony Formation" section), the smaller field of view impaired our ability to conduct cell counting and tracking analyses. As a compromise, all major experiments were performed using a 10× objective (cf. "Time-Lapse Live Cell Imaging" section). Lastly, note that for reasons to be discussed in "Substrate Displacements During Colony Formation" section, measured substrate displacements were *not* used to calculate/estimate the associated cellular tractions as is typically done in a TFM experiment.[33]

Immunofluorescence

In a separate but parallel set of experiments, keratinocytes were cultured in *Low* Ca^{2+} on both *soft* and *stiff* PA gels that were fabricated on 12 mm coverslips for immunofluorescent labeling of either actin microfilaments and E-cadherin; keratin intermediate filaments and desmoplakin; integrins $\beta1$ and $\beta4$; or involucrin. Labeling was performed in accord with protocol modified from Zamansky[43] and Selby.[32] After seeding and allowing the cells to equilibrate for three hours, the calcium levels of the culture medium were increased to *High* Ca^{2+} for selected specimens. At times $t = 0$ min, 1, 4, and 24 h following the calcium switch, keratinocytes were removed from culture and fixed with either cold (−20 °C) methanol for 10 min (actin and E-cadherin; keratin and desmoplakin) or 4% paraformaldehyde at room temperature for 1 h ($\beta1$ and $\beta4$; involucrin). Samples in which the calcium concentration was initialized and maintained at 0.09 mM throughout culture (*Low* Ca^{2+}) were also removed from culture and fixed at 0 and 24 h. Fixative was then removed and the samples were washed with PBS. Samples that were fixed with 4% paraformaldehyde were further permeablized with 0.5% Triton-X for 5 min and washed in PBS for 10 min. All samples were then blocked for 30 min with either 10% normal goat serum or 10% normal donkey serum and incubated at 37 °C using the following antibody combinations: (i) a 1:100 dilution of rabbit anti-cytokeratin polyclonal antibodies (#BT-571, Biomedical Technologies, Ward Hill, MA) and a 1:100 dilution of mouse anti-desmoplakin I + II monoclonal antibodies (#AB16434, Abcam); (ii) a 1:100 dilution of mouse anti-actin monoclonal antibodies (#MAB1501R, EMD Millipore, specific for both globular and filamentous actin) and a 1:100 dilution of rabbit anti-E cadherin monoclonal antibodies (#AB40772, Abcam); (iii) a 1:100 dilution of goat anti-integrin $\beta1$ polyclonal antibodies (#SC6622, Santa Cruz Biotechnology) and a 1:100 dilution of mouse anti-human CD104 (i.e., integrin $\beta4$) monoclonal antibodies (#555722, BD Pharmingen); and (iv) a 1:500 dilution of mouse anti-involucrin monoclonal antibodies (#AB68, Abcam). Anti-involucrin antibodies were allowed to incubate for 2 h at 37 °C as opposed to the 1-h incubation used for the other antibody combinations. Following incubation, samples were treated with a second blocking step in either 10% normal goat serum or 10% normal donkey serum for a period of 20 min. Finally, the coverslips were incubated for 30 min at 37 °C with a 1:100 dilution of the corresponding secondary antibodies: goat anti-rabbit IgG antibodies (#A-11034, Invitrogen Corporation), goat anti-mouse IgG antibodies (#A-11031, Invitrogen Corporation), donkey anti-goat IgG H&L antibodies (#AB150129, Abcam), or donkey anti-mouse IgG antibodies (#A10036, Life Technologies). Between each step in the process, all samples were washed with PBS. Finally, coverslips were mounted onto microscope slides with Prolong® Gold Antifade Mountant with DAPI (Life Technologies) in order to visualize keratinocyte nuclei. Immunofluorescence images were acquired using a Nikon Eclipse Ti inverted microscope with a 20× CFI Plan Apo DIC objective and a 1.5× magnifier.

Statistical Analysis

Statistical significance ($p < 0.05$) was determined by performing either Student's t tests when comparing two groups or analysis of variance (ANOVA) when comparing multiple groups. All statistical analysis was done in MATLAB.

RESULTS

Kinematics of Keratinocyte Migration and Colony Formation

Differences in keratinocyte behavior and colony formation as a function of substrate stiffness and exposure to *Low* Ca^{2+} (0.09 mM) and *High* Ca^{2+} (1.2 mM) medium were assessed by imaging and tracking keratinocyte migratory behaviors on pepsin digested type I collagen coated *soft* and *stiff* PA gels. Over the 24-h observation period, several behavioral differences were observed (Movie S1–S4).

First, keratinocytes were significantly more spread out on *stiff* substrates compared to *soft*. Significant differences in spread areas between keratinocytes on *soft* and *stiff* substrates in our *Low* Ca^{2+} control experiments were observed for all analyzed time points (Table 1). For example, at $t = 2$ h, the average area of a single keratinocyte maintained in our *Low* Ca^{2+} control experiments on *soft* vs. *stiff* gels was 535 ± 315 μm^2 ($n = 18$) and 3189 ± 2119 μm^2 ($n = 16$), respectively. In our *High* Ca^{2+} experiments, a two-way ANOVA suggests that keratinocyte spread area is a function of both time and substrate stiffness, with increased spread areas on *stiff* compared to *soft* substrates, and a general trend of decreasing spread areas with duration of culture for both types of substrate (Table 1). In comparing differences between spread areas in *High* Ca^{2+} and *Low* Ca^{2+} experiments, we did find that the calcium switch had an effect on spread area during the first several hours of culture on *soft* gels (but not *stiff* gels), but the significance was lost at later time points.

With regard to migration velocities (Table 2), in *Low* Ca^{2+} medium, keratinocytes were 30% faster on *soft* gels, with an average instantaneous velocity of 1.13 ± 0.25 μm/min compared to 0.86 ± 0.27 μm/min on *stiff* gels ($p < 0.005$). Velocities remained virtually unchanged upon exposure to *High* Ca^{2+} medium (1.11 ± 0.41 μm/min on *soft* gels and 0.85 ± 0.39 μm/min on *stiff* gels) across all time points, demonstrating that keratinocyte speed was *not* affected by the calcium switch.

In contrast, the process of colony formation was dependent on the switch to *High* Ca^{2+} medium (Tables 2, 3; Fig. 1). On both types of PA gel, pairs of keratinocytes in *Low* Ca^{2+} medium frequently came into contact with each other, but they did not form permanent attachments, and they ultimately disengaged from each other on time scales ranging from a few minutes to several hours over the 24-h observation period. The duration of engagement (Table 3), though not significantly different ($p = 0.1454$), was generally shorter on *soft* gels (average of 53 ± 99 min, median 23 min) than on *stiff* gels (average of 100 ± 120 min, median 46 min). Changing to *High* Ca^{2+} medium triggered the keratinocytes to join colonies that were marked by the formation of more permanent cell–cell adhesions, consisting of both desmosomes (Fig. 5) and adherens junctions (Fig. 6). This process unfolded in a dynamic substrate-dependent manner, with keratinocytes joining and sometimes releasing from each other until the majority of cells in the field were associated with couples or colonies. On *soft* gels, the number of single keratinocytes in a field quickly decreased from an average of 24.3 ± 4.7 cells (or $87.6 \pm 13.6\%$ of total cells in the field) at $t = 0$ h to 3.7 ± 2.5 cells ($10.8 \pm 7.8\%$) at $t = 24$ h (Table 3). The number of single keratinocytes on *stiff* gels did not decrease as quickly or to the same extent (31.0 ± 5.3 to 6.0 ± 4.0 cells or $97.7 \pm 4.0\%$ to $21.5 \pm 12.2\%$ over the same range). A two-way ANOVA indicated that the number of single cells was dependent on both time and substrates stiffness ($p < 0.001$), whereas the average total number of keratinocytes per visual field for the *soft*

TABLE 1. Keratinocyte spread areas.

	Cell area ($\times 10^3$ μm^2)						
Condition	0 h	1 h	2 h	4 h	8 h	16 h	24 h
Low Ca^{2+}							
Soft	0.96 ± 0.64	1.06 ± 0.52	0.54 ± 0.32	0.62 ± 0.37	0.51 ± 0.22	0.74 ± 0.41	0.42 ± 0.13
Stiff	3.23 ± 1.31	3.54 ± 1.71	3.19 ± 2.12	2.33 ± 1.27	2.57 ± 1.83	2.08 ± 1.44	2.15 ± 1.58
High Ca^{2+}							
Soft	1.41 ± 0.85	1.55 ± 1.05	0.96 ± 0.73	0.96 ± 0.73	0.96 ± 0.87	0.57 ± 0.21	0.56 ± 0.13
Stiff	3.17 ± 1.59	2.76 ± 1.56	2.94 ± 2.02	2.58 ± 2.09	1.99 ± 1.02	1.99 ± 1.37	1.85 ± 1.50

Data are mean ± SD.

TABLE 2. Keratinocyte migration and colony forming metrics.

	Low Ca^{2+}		High Ca^{2+}	
Measurement	Soft	Stiff	Soft	Stiff
Keratinocyte speed (μm/min)	1.13 ± 0.25	0.86 ± 0.27	1.11 ± 0.41	0.85 ± 0.39
Duration of cell engagement (min)	53 ± 99	100 ± 120	152 ± 155	219 ± 157
$t_{50\%}$ (min)	–	–	57.3 ± 22.7	162.7 ± 74.9
t_{first} (h)	–	–	4.5 ± 2.7	11.7 ± 5.5
Distance rank (DR)	–	–	2.6 ± 2.8	5.7 ± 5.5
RC—125 μm (% of cells that attached)	–	–	77.8 ± 4.9	51.7 ± 12.1
RC—175 μm (% of cells that attached)	–	–	64.8 ± 2.8	40.3 ± 10.9

Data are mean ± SD.

TABLE 3. Keratinocyte classification and counts.

		Time						
Condition	Measurement	0 h	1 h	2 h	4 h	8 h	16 h	24 h
High Ca^{2+}								
Soft	No. single	24.3 ± 4.7	19.0 ± 1.7	13.3 ± 4.0	9.7 ± 1.5	7.3 ± 1.5	4.7 ± 2.1	3.7 ± 2.5
(n = 3)	No. couples	0.7 ± 1.2	1.7 ± 0.6	1.7 ± 0.6	1.7 ± 0.6	1.3 ± 1.2	1.7 ± 0.6	1.7 ± 0.6
	No. colonies	0.7 ± 0.6	1.7 ± 0.6	3.0 ± 1.0	2.3 ± 1.5	4.3 ± 1.2	4.0 ± 0.0	4.7 ± 1.2
	No cells per colony	2.0 ± 1.7	3.2 ± 1.4	3.3 ± 1.2	5.1 ± 2.6	4.9 ± 2.2	6.3 ± 3.3	6.1 ± 3.2
Stiff	No. single	31.0 ± 5.3	26.3 ± 6.1	24.0 ± 3.6	21.3 ± 5.9	12.3 ± 6.6	7.7 ± 2.1	6.0 ± 4.0
(n = 3)	No. couples	0.3 ± 0.6	1.7 ± 1.5	2.7 ± 0.6	2.3 ± 2.1	5.3 ± 3.5	2.3 ± 1.5	3.0 ± 2.0
	No. colonies	0.0 ± 0.0	0.3 ± 0.6	0.7 ± 0.6	2.0 ± 1.7	3.3 ± 1.5	3.3 ± 0.6	3.0 ± 1.0
	No cells per colony	0.0 ± 0.0	1.0 ± 1.7	2.3 ± 2.1	3.2 ± 0.4	3.4 ± 0.5	4.0 ± 1.3	5.2 ± 2.3
Low Ca^{2+}								
Soft	No. single	28	28	23	21	23	22	25
(n = 1)	No. couples	0	0	2	3	0	0	0
	No. colonies	0	0	0	0	1	0	0
	No cells per colony	0	0	0	0	3	0	0
Stiff	No. single	21	22	21	20	20	20	22
(n = 1)	No. couples	2	0	0	0	1	2	3
	No. colonies	0	1	1	0	0	1	1
	No cells per colony	0	3	3	0	0	4	4

Data are mean ± SD.

and *stiff* gels remained statistically constant throughout the duration of the experiment at 32.1 ± 4.7 and 29.8 ± 5.7 cells, respectively ($p = 0.57$).

In *High* Ca^{2+}, when two keratinocytes joined together on a *soft* gel, the couple that formed generally did not last long (152 ± 155 min, median 88 min) because either the cells released from each other and continued on as single cells or other cells quickly joined the couple to form a colony. In contrast, keratinocytes on *stiff* gels formed couples that endured longer (219 ± 157 min, median 198 min). The number of couples did not change significantly over time on either gel (Table 3). There was, however, a significant dependence on substrate stiffness ($p < 0.001$), with roughly twice as many couples found on *stiff* gels (3.3 ± 1.0 couples, or 21.7 ± 5.8% of the total cells) as were found on *soft* gels (1.5 ± 0.3 couples, or 10.6 ± 2.8%). It should be noted that a small number of couples ($n = 3$ on *soft* gels, $n = 4$ on *stiff* gels) persisted for the duration of the experiment and were excluded from these calculations.

The vast majority of keratinocytes on both types of PA gel ultimately formed colonies, with significantly more colonies (3.8 ± 1.0 vs. 2.9 ± 1.3, $p < 0.001$) and more cells per colony (5.4 ± 1.2 and 3.6 ± 1.2, $p < 0.001$) forming on *soft* rather than *stiff* gels, using keratinocyte counts averaged over the duration of the experiment (Fig. 1). At the conclusion of the experiment ($t = 24$ h), the same trends were observed with 4.7 ± 1.2 colonies vs. 3.0 ± 1.0 colonies and 6.1 ± 3.2 cells per colony vs. 5.2 ± 2.3 cells per colony observed on *soft* vs. *stiff* gels, respectively. Colonies also formed faster on *soft* gels. Two metrics were used to characterize the *rate* of colony formation (Table 2). First, the average time, t_{first}, required for the first colony to form (excluding colonies already formed at $t = 0$) was calculated. It was found that the first colony formed faster (but not significantly, $p = 0.08$) on *soft* gels (57.3 ± 22.7 min) than on *stiff* gels

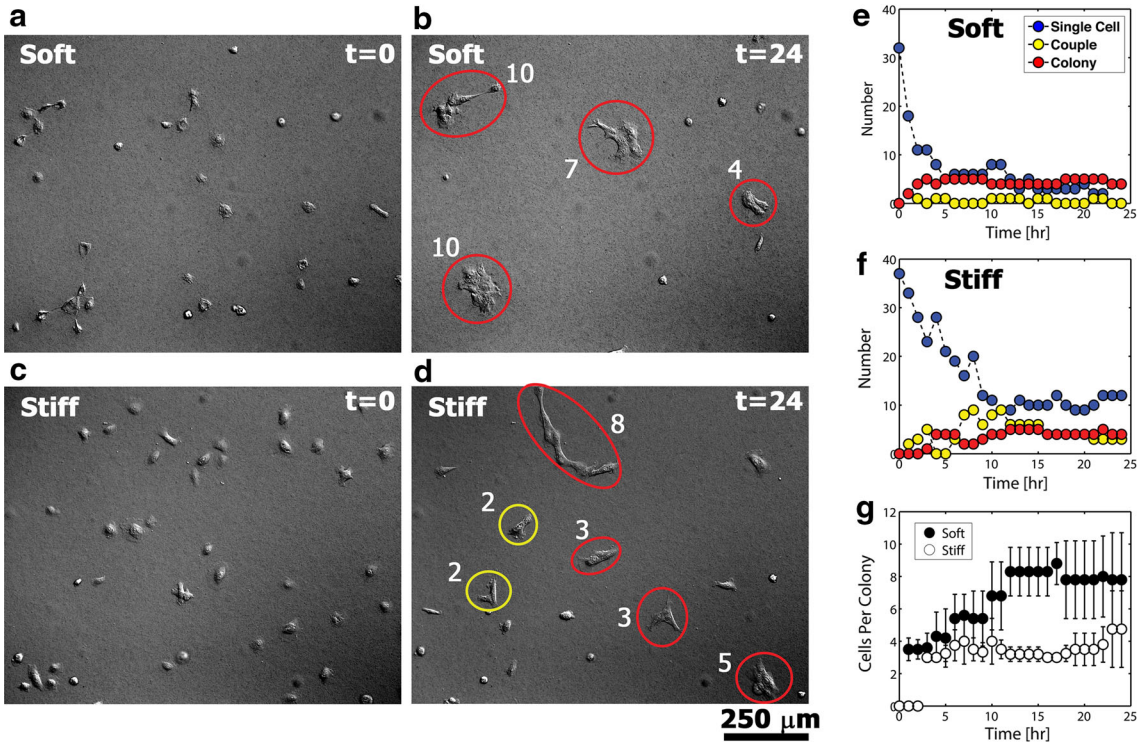

FIGURE 1. Representative DIC images showing differences in colony formation on *soft* and *stiff* PA gels at $t = 0$ h (a, c) and $t = 24$ h (b, d). At each hour the number of single cells, couples (yellow ellipses), and colonies (red ellipses) was determined (e, f), along with (g) the number of cells per colony (number adjacent to each ellipse).

(162.7 ± 74.9 min). The second metric calculated was the average time, $t_{50\%}$, required for at least 50% of the keratinocytes in the image to associate with a colony. This time also was shorter on *soft* compared to *stiff* gels at 4.5 ± 2.7 and 11.7 ± 5.5 h, respectively, though again, not significantly ($p = 0.1115$).

In general, keratinocytes did not always form couples or colonies through mechanical contacts with their closest neighboring cells, an unexpected behavior that was particularly evident for cells cultured on *stiff* gels. To quantify this difference in keratinocyte behavior observed during the process of colony formation on *soft* vs. *stiff* substrates, we defined an *ad hoc* analysis termed the DR. When ranked ordered by the magnitudes of their respective internuclear separations, keratinocytes cultured on *stiff* gels formed couples or colonies with neighboring cells that had an average DR of 5.7 ± 5.5, median rank of 4, compared to an average DR on *soft* gels of 2.6 ± 2.8, median rank of 2 (Table 2).

In addition to the *ordinal* DR metric, we performed a second *ad hoc* analysis, termed the RC, in an attempt to correlate the length scale of a cell with the degree of cooperativity in colony formation characterized by keratinocytes cultured on *soft* vs. *stiff* substrates. Based on observed cell spread areas at time $t = 0$ (Table 1) for *High* Ca^{2+} conditions, we estimated *nominal* cell diameters (assuming circular spread areas) of ~40 and ~60 μm for keratinocytes cultured on *soft* and *stiff* substrates, respectively. Then, assuming a stiffness-independent mean *nominal* cell diameter of ~50 μm and hence a *nominal* cell couple diameter of ~100 μm, RC analysis was performed for radii of 125 and 175 μm, or ~1.5 and ~2.5 nominal cell diameters, respectively, from the peripheral margin of a hypothetical cell couple of interest (Table 2; Fig. 2). Keratinocytes joined with 77.8 ± 4.9% of the cellular entities (single cells, couples, or colonies) present within a 125 μm RC on *soft* gels, compared to 51.7 ± 12.1% for the same 125 μm RC on *stiff* gels ($p < 0.03$). Similarly, keratinocytes joined with 64.8 ± 2.8% of the cellular entities present within a 175 μm RC on *soft* gels, compared to 40.3 ± 10.9% for the same 175 μm RC on *stiff* gels ($p < 0.019$).

Substrate Displacements During Colony Formation

In addition to keratinocyte morphology and kinematics, differences in substrate deformations were also observed between keratinocytes cultured on *soft* vs. *stiff* substrates. Under both *High* Ca^{2+} and *Low* Ca^{2+} conditions, keratinocytes cultured on *stiff* PA gels generated very small substrate displacements, as monitored by tracking the positions of embedded

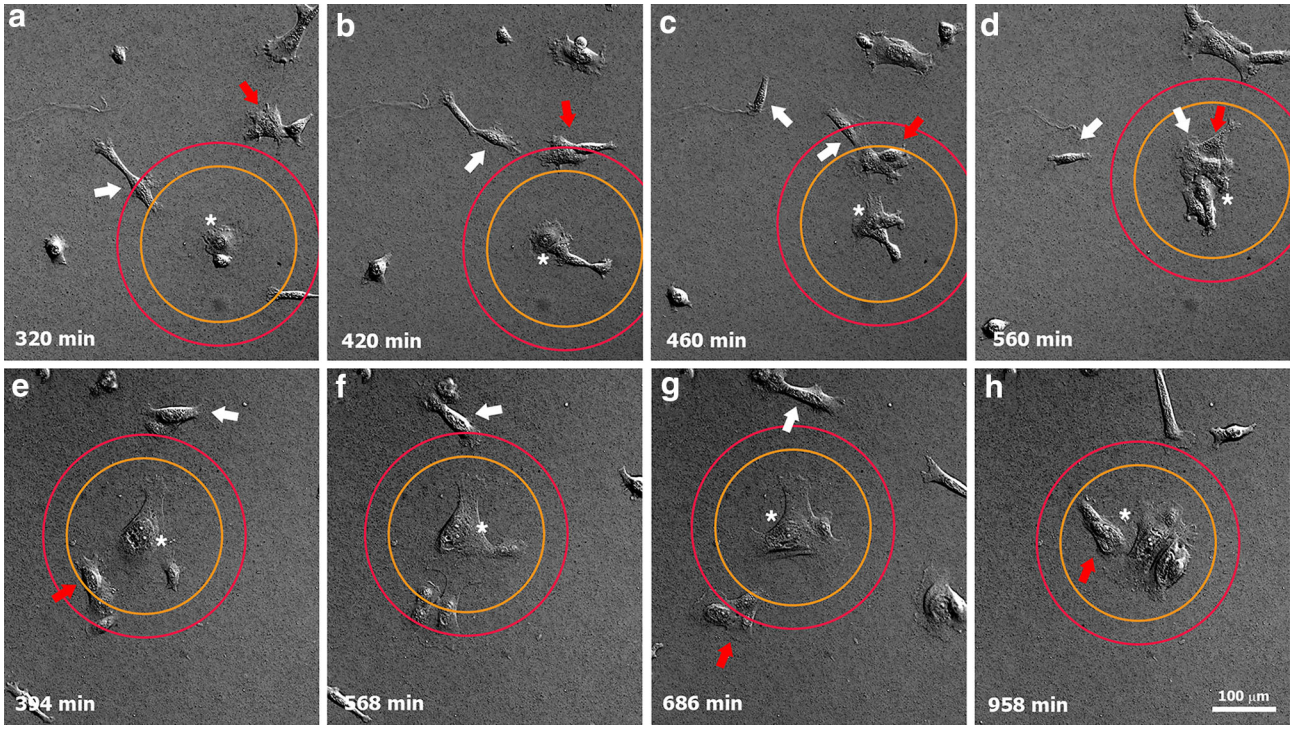

FIGURE 2. Representative images showing single keratinocytes, couples, and colonies entering the RC for radii of 125 μm (orange circle) and 175 μm (red circle) on *soft* (a–d) and *stiff* PA gels (e–f). The couple/colony analyzed in each example is indicated by an asterisk. On the *soft* gel (a–d), an approaching couple (white arrow) crosses the inner and outer RC at *t* = 320 min in close proximity to a small colony (red arrow) that just touches the outer RC. As the colony migrates into the inner RC at *t* = 420 and *t* = 460 min, keratinocytes of the first couple disengage from one another (two separate white arrows). One cell eventually exits the outer RC and the other cell merges with the entering colony (red arrow) to join the central colony (asterisk) at time *t* = 560 min. On a *stiff* gel (e–h), a small colony (red arrow) is present at the inner RC, and a cell couple (white arrow) is present at the outer RC at *t* = 394 min. The couple eventually exits both RC (leaving the field of view) without joining the central couple of interest (asterisk), while the small colony (red arrow) temporarily moves away from the couple of interest at *t* = 568 min and *t* = 686 min before finally merging with it at *t* = 958 min to form a small colony.

fluorescent microspheres. The single largest tracked displacement using a 10× objective (Movie S4) was 1.6 μm—a value below the estimated 2.7 μm algorithm measurement error at this magnification. Consequently, the microsphere displacements on *stiff* gels at this magnification were treated as effectively zero, and no further quantitative analysis was conducted. Adjunctive experiments performed on a *stiff* PA gel using a 20× objective with a 1.5× magnifier resulted in an average maximum displacement per time point of 1.39 ± 1.93 μm (0.62 μm estimated algorithm error), with 2.29 μm representing the single largest maximum displacement measured over the 24-h duration of the experiment (Movie S6). These observations confirmed that small but measureable substrate displacements were generated by keratinocytes cultured on *stiff* substrates. However, at this magnification the field of view was markedly reduced, and ultimately deemed too restrictive for assessing *collective* keratinocyte behaviors during the process of colony formation.

For keratinocytes cultured on *soft* gels maintained in *Low* Ca^{2+} conditions as controls, microsphere displacements were much higher, but did not vary much over the 24-h time course (Fig. 3, Movie S1). The overall average microsphere displacement was 4.2 ± 2.6 μm, with 17.9 μm representing the single largest microsphere displacement tracked. Under *High* Ca^{2+} conditions, keratinocytes generated microsphere displacements that were not only higher, but they also increased with duration of culture and in parallel with nascent epithelial sheet formation (Figs. 3, 4, Movie S3). Average displacements ranged from 8.7 ± 5.7 μm at $t = 0$ h to 19.4 ± 21.2 μm at $t = 24$ h (Movie S7). Here, the single largest displacement tracked was 113.5 μm, occurring at $t = 24$ h.

Two important experimental factors precluded quantitative TFM analysis in our study, namely: (i) limitations in the detection and tracking of substrate displacements for our *extremes* in substrate stiffness, and (ii) the ill-defined and dynamic nature of the boundary conditions required to solve the inverse problem of calculating cell tractions from measured substrate displacements. With regards to the former, the *soft* and *stiff* formulations of our PA gels were not optimized for TFM analysis: substrate displacements

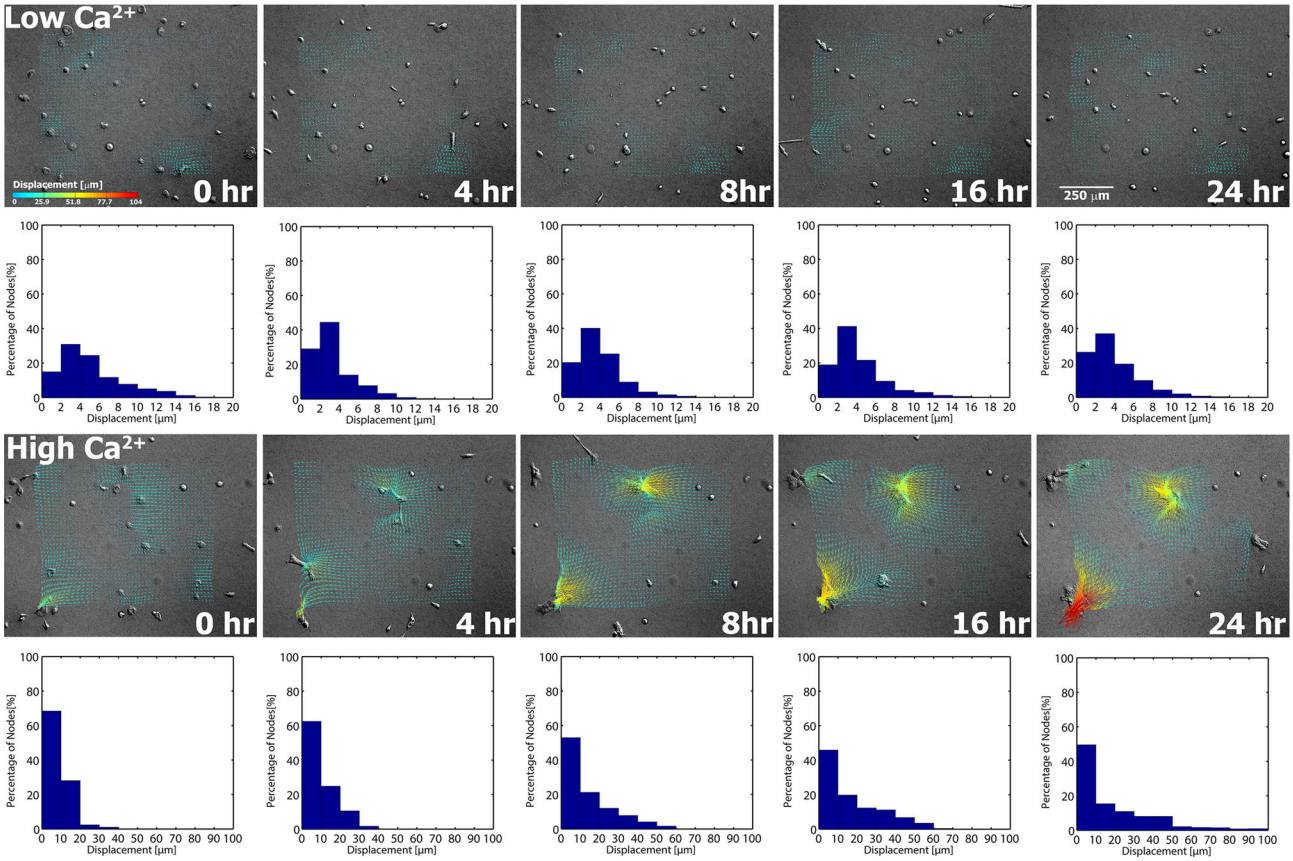

FIGURE 3. Cell tractions deform *soft* PA gels in a manner that is dependent on the calcium concentration of the culture medium and the extent of keratinocyte colony formation. Substrate displacements are determined by tracking microsphere displacements in *Low* Ca^{2+} and *High* Ca^{2+} experiments at the indicated time points (cf. "Substrate Displacement Tracking" section). Displacements increase with time under *High* Ca^{2+} conditions, correlating with the extent of keratinocyte colony formation. Note the difference in the range of *x*-axis displacements indicated on the histograms associated with the *Low* Ca^{2+} and *High* Ca^{2+} measurements.

observed in our *stiff* gels were so small that they fell within the uncertainty of our tracking algorithms, while the extremely large displacements observed in our *soft* gels invalidate many of the assumptions inherent to most forms of TFM analysis (infinitesimal strains and a linear elastic continuum). With regards to boundary conditions, note that keratinocytes were free to migrate in and/or out of the optical field of view throughout the 24-h duration of our experiment. Thus, not only are the cellular tractions present at the boundaries of our observation window spatially uncertain, they are also temporally variable. These technical issues will be addressed in future work by using smaller cell numbers, more focused fields of view with higher power objectives, and TFM analysis that employs a large deformation formulation.[34]

Keratinocyte Cytoskeletal Morphology

Immunofluorescent labeling of actin microfilaments, keratin intermediate filaments, desmoplakin (component of desmosomes), and E-cadherin (component of adherens junctions) within keratinocytes cultured on both *soft* and *stiff* PA gels revealed differences in cytoskeletal organization that were consistent with the dynamic cell morphologies observed in our time-lapse DIC images (Figs. 5, 6). In *Low* Ca^{2+} conditions ($t = 0$ h), keratinocytes on both *soft* and *stiff* substrates assumed a predominantly rounded morphology, with cells on *stiff* substrates exhibiting a notably increased degree of cell spreading. Spindled morphologies were also observed, with an increased number density on *soft* compared to *stiff* substrates. With respect to our time-lapse DIC images, small rounded keratinocytes were observed to migrate over the surface of both types of gel, occasionally transitioning into an elongated spindled morphology before eventually condensing back into a rounded morphology and resuming their migratory behaviors (cf. $t = 2$ h of Movie S1). This type of transitional morphologic behavior, though present, was relatively uncommon on *stiff* gels. Following 24 h of culture in

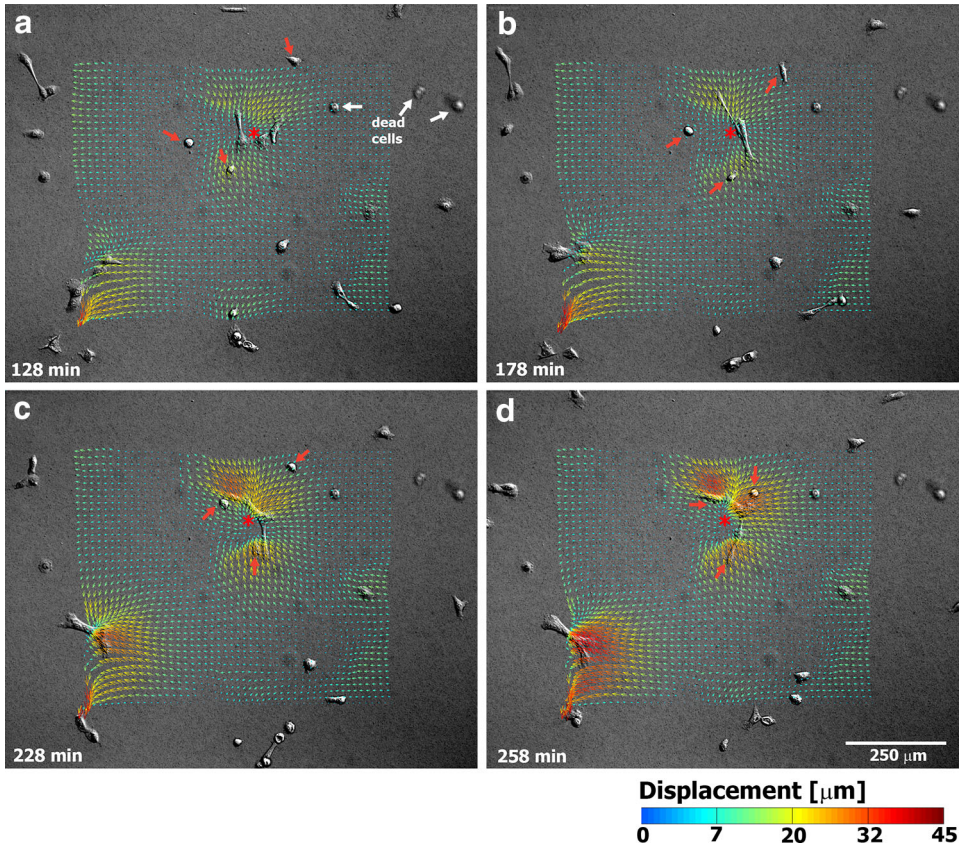

FIGURE 4. Selected frames show that in *High* Ca^{2+} conditions, keratinocyte colonies forming on *soft* PA gels generate large substrate displacements that appear to draw single keratinocytes inward towards a forming colony. Dead cells are indicated by white arrows. The relative positions of three selected individual keratinocytes are indicated by red arrows at all four time points with respect to a forming colony (indicated by an asterisk).

Low Ca^{2+} conditions, the number of keratinocytes adopting a small rounded-up morphology was dramatically increased on *soft* compared to *stiff* substrates.

For both substrate types under *Low* Ca^{2+} conditions, focal actin concentrations were noted at the cell peripheries, with thicker actin fibers indicative of stress fibers more clearly visualized in keratinocytes cultured on *stiff* substrates across all time points. At baseline ($t = 0$ h, *Low* Ca^{2+}), keratin intermediate filaments formed networks that centrifugally extended from a perinuclear cage-like structure. Following the calcium switch, microfilament organization within keratinocytes cultured on *soft* PA gels changed rapidly, marked by the formation of lamellipodial- and pseudopodial-like structures at $t = 1$ h. At $t = 24$ h following the calcium switch, cell–cell adherens junctions were formed between keratinocytes within colonies on both *soft* and *stiff* substrates, as marked by the punctate/linear staining of E-cadherin (Fig. 6). Within this same time frame, keratin intermediate filaments reorganized to form highly integrated networks that spanned multiple cell-to-cell contacts within colonies cultured on both *soft* and *stiff* substrates. These networks were associated with the formation of cell–cell desmosomes, as marked by the punctate staining pattern of desmoplakin (Fig. 5). Desmoplakin staining appeared more prominent on *stiff* vs. *soft* substrates at $t = 4$ h, suggestive of an increased rate of desmosome assembly.

Interestingly, keratinocytes found along the periphery of colonies cultured on *soft* substrates exhibited a spindled morphology with visible lamellipodial- and pseudopodial-like microfilament structures, suggestive that colonies on *soft* substrates are more actively seeking mechanical contact(s) with neighboring cells or colonies in order to incorporate them into the evolving epithelial sheet. Similar pseudopodial-like extensions were also observed in some single keratinocytes that were in close proximity to a nearby colony. By correlation, in our time-lapse DIC images (Fig. 7), single keratinocytes on *soft* gels were frequently observed to extend pseudopodial-like structures that were directed towards the colony it was attempting to join. In contrast to these findings, keratinocytes present along the periphery of colonies cultured on *stiff* substrates exhibited a more rounded morphology with little to no

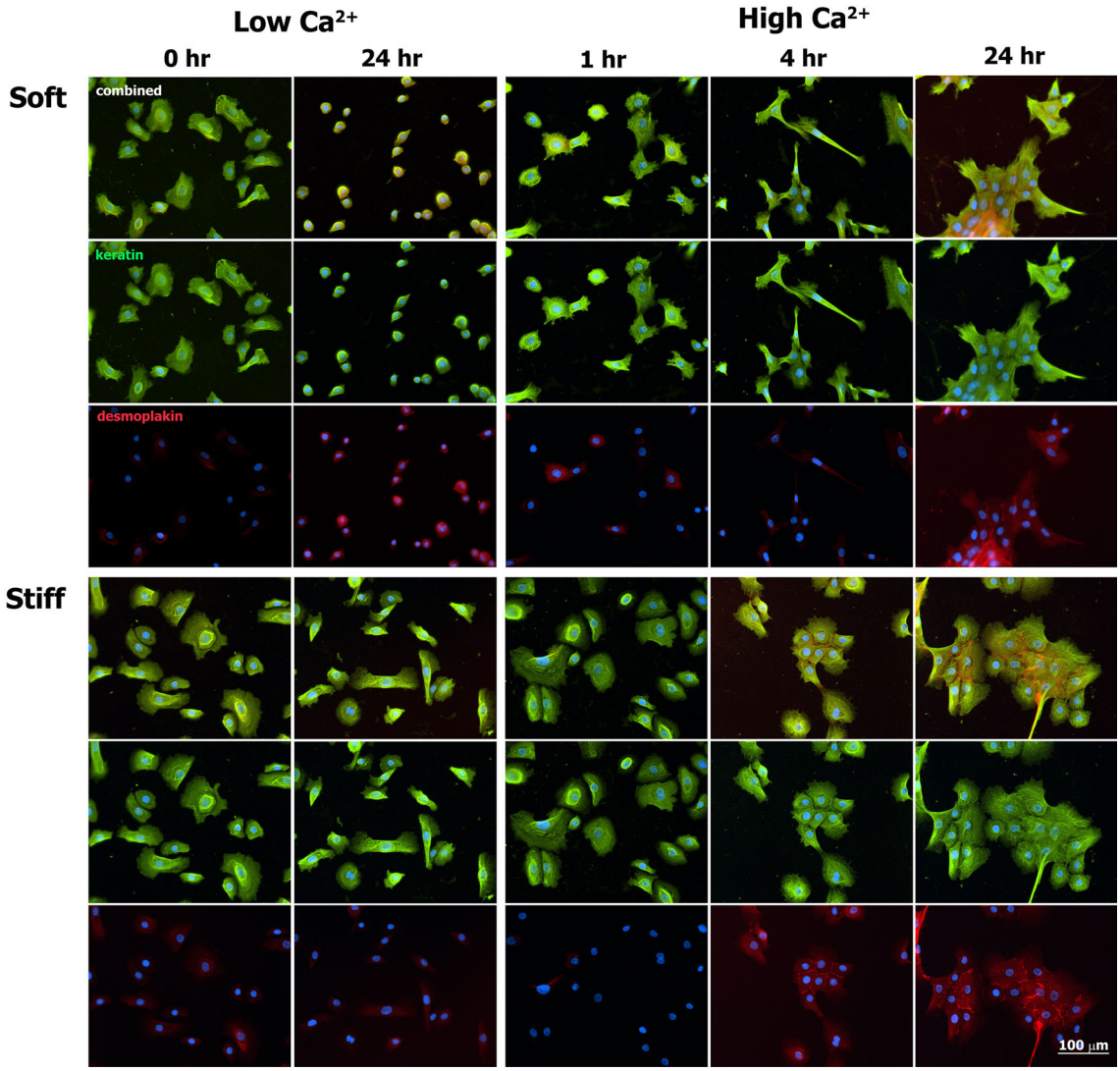

FIGURE 5. Immunofluorescence images of keratin intermediate filaments (green), desmoplakin (red), and nuclei (blue) in normal human epidermal keratinocytes culture for select times on *soft* and *stiff* PA gels exposed to both *Low* Ca^{2+} and *High* Ca^{2+} conditions.

evident formation of pseudopodial-like microfilament structures. As noted in our DIC images, keratinocytes on *stiff* substrates frequently did not join a colony *via* directed orthogonal movements, but rather seemed to merge with its eventual colony *via* an increasingly tangential approach (Fig. 7).

In order to explore possible differences in cell–matrix adhesive contacts under various experimental conditions, immunofluorescence experiments (Fig. 8) were performed by co-labeling for β1 integrin, a component of focal adhesion contacts, and β4 integrin, a component of hemidesmosomes *in vivo* and hemidesmosome-like contacts *in vitro*.[37] Under *Low* Ca^{2+} conditions, some staining of β1 integrin was observed over 24 h of culture, whereas β4 integrin was diffusely expressed throughout the cytoplasm without any definitive foci of staining along the cell–matrix interface. After 24 h of culture under *High* Ca^{2+} conditions, punctate foci of β1 integrin staining were observed in all keratinocytes belonging to a colony, independent of a given cell's position within the colony and independent of the stiffness of the PA gel. Staining for β4 integrin remained cytoplasmically diffuse in cells cultured on *stiff* PA gels for all time points. At $t = 24$ h following the calcium switch, punctate staining of β4 integrin along the cell–matrix interface appeared within keratinocytes positioned along the periphery of colonies cultured on *soft* substrates (Fig. 9a). This staining pattern was *not* observed within colonies cultured on *stiff* gels (Fig. 9b).

Lastly, the average internuclear spacing of keratinocytes within colonies cultured under *High* Ca^{2+} condi-

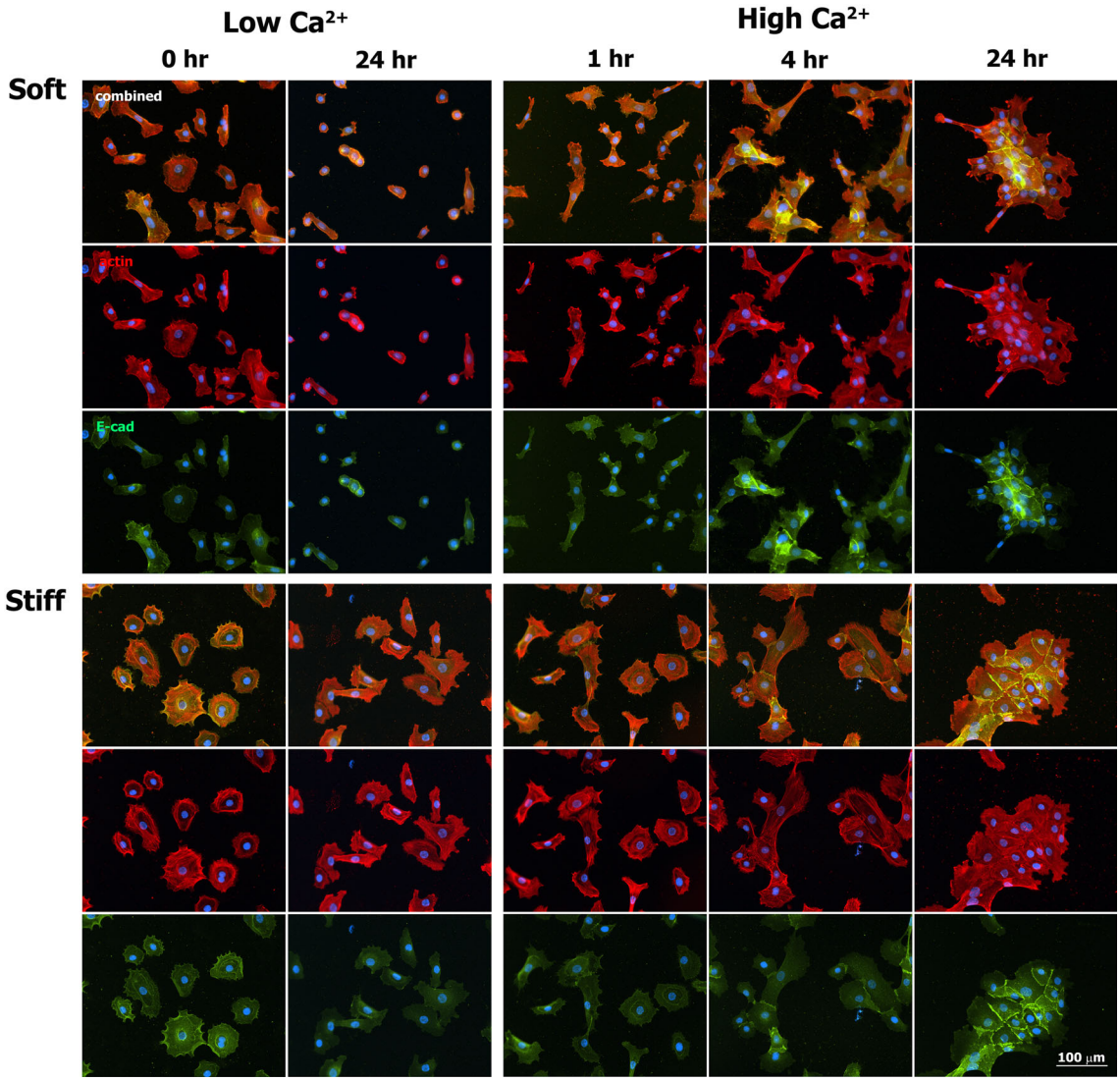

FIGURE 6. Immunofluorescence images of actin (red), E-cadherin (green), and nuclei (blue) in normal human epidermal keratinocytes culture for select times on *soft* and *stiff* PA gels exposed to both *Low* Ca^{2+} and *High* Ca^{2+} conditions.

tions on *soft* substrates was diminished compared to the internuclear spacing of cells on *stiff* substrates. In some instances, this reduction in spacing might be due to the local three-dimensional stratification and differentiation of keratinocytes within the colony, as can be inferred from partially overlapping DAPI-stained nuclei (Figs. 5, 6, *soft* substrate, $t = 24$ h). In order to evaluate whether substrate-dependent keratinocyte differentiation played a role in the colony-forming behavior observed in our experiments, we also evaluated involucrin expression, a keratinocyte-specific differentiation marker,[39] across select time points of culture under both *Low* Ca^{2+} and *High* Ca^{2+} conditions (Fig. 10). Under *Low* Ca^{2+} conditions, positive staining for involucrin was noted at $t = 24$ h for a very small subset of cells cultured on both *soft* and stiff PA gels. At $t = 4$ and $t = 24$ h following the calcium switch, positive involucrin staining was observed within keratinocytes cultured on both *soft* and *stiff* gels, with staining primarily localized to cells positioned within the center and stratified layers of each given colony. Involucrin staining was notably absent from peripheral cells of the colony and keratinocytes migrating as single cells. No definitive differences in involucrin staining were noted between *soft* and *stiff* gels.

DISCUSSION

In qualitative agreement with Pelham's and Wang's seminal observations of the migratory behaviors of 3T3 fibroblasts and rat kidney epithelial cells (NRK-

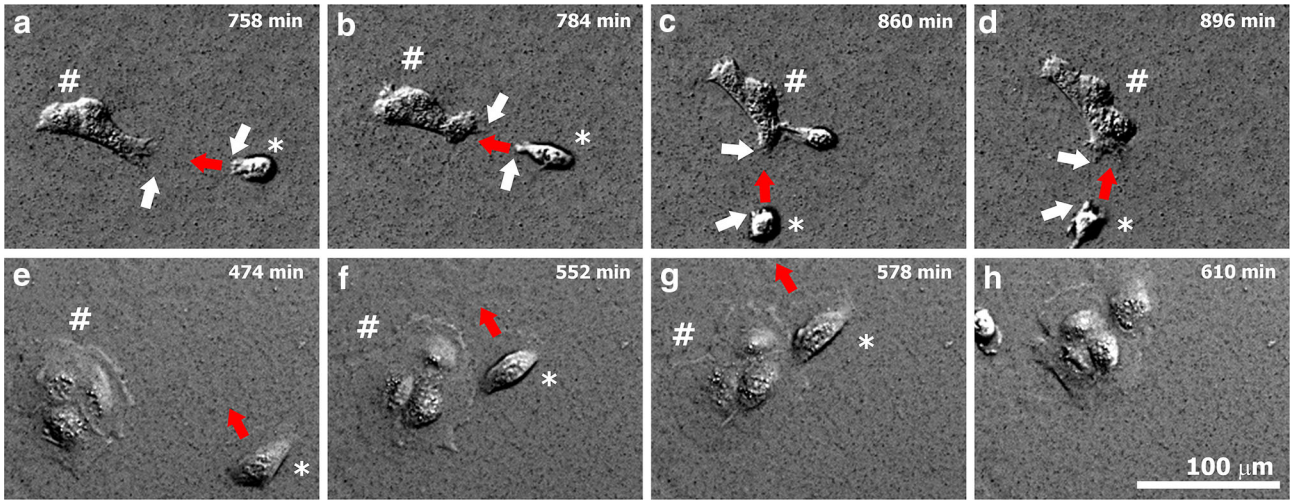

FIGURE 7. The characteristics of colony formation differ on *soft* (a–d) and *stiff* (e–h) gels. On *soft* gels (a–d), small pseudopodial-like projections (white arrows) extend outward from both the approaching cell (indicated by an asterisk) and its eventual cell of contact (indicated by number sign) within the colony. The approaching cell migrates directly (velocity vector indicated by red arrows) towards its contact cell in a process that appears to be mediated by these pseudopodial-like extensions. On *stiff* gels (e–h), pseudopodial-like projections were not observed between merging keratinocytes during the process of colony formation. Rather, migrating keratinocytes (asterisk) often approached their eventual cell of contact within a colony (number sign) *via* an almost tangential pathway, as can be seen by the velocity vectors (red arrows) indicated for the approaching keratinocyte labeled in (e), (f), and (g) that eventually joins the colony shown in (h).

52E),[25] our experiments showed that normal HEKn exhibit smaller spread areas but increased migration velocities when cultured on *soft* as opposed to *stiff* substrates. When compared to normal human keratinocytes cultured on type I collagen attached to an *in vitro* "observation chamber" (1.2 ± 0.7 μm/min; exact substrate material not specified), our observed migration velocities are strikingly similar in magnitude.[15] In quantitative agreement with the experiments performed by Trappmann *et al.*,[35] we observed similar keratinocyte spread areas on our nominal 1.2 kPa *soft* PA gels compared to their 0.5 kPa Pa gels. Additionally, the transient spindled morphologies we observed in keratinocytes cultured on our *soft* gels were also observed by Trappmann *et al.* in keratinocytes cultured on their 2 kPa gels.

Collectively, the effects of substrate stiffness on spread areas and migration velocities that we observed in our keratinocyte studies are in agreement with prior studies that utilized cells of both parenchymal and mesenchymal origin. Some have argued that these general observations can be attributed to the weak/unstable nature of focal contacts associated with cells cultured on *soft* substrates.[25,26] Interestingly, for fibroblasts, the apparent dependence on bulk substrate stiffness seems to disappear when cells are cultured on fibrous matrix.[42] Trappmann *et al.* have reported a similar finding with cultured keratinocytes, proposing that cells respond to feedback from the mechanical tethering of individual near-field matrix fibers as opposed to any bulk mechanical property of the substrate.[35] More recently, Wen *et al.* have reported that the differentiation of adipose-derived and bone marrow-derived stromal cells is regulated by matrix stiffness in a manner that is independent of protein tethering.[41] Given the apparent discrepancies among these various studies, we pose that the mechanobiological mechanism by which keratinocytes sense and respond to perturbations in their mechanical environment remains an open question ripe for further investigation.

Although the migration rates of fully-formed keratinocyte *sheets* have been observed to be dependent on substrate stiffness,[38] to the best of our knowledge, our work represents the first studies that have documented the effect of substrate stiffness on the migration velocities of *individual* HEKn. Wang *et al.* cultured HaCaT epidermal cells (an immortalized human keratinocyte cells line) on polydimethylsiloxane (PDMS) substrates that were 16, 20, and 200 kPa in nominal stiffness. Using what is often referred to as a *scratch assay*, they found that a fully-formed keratinocyte sheet migrates to close an artificially created defect in the sheet at a faster rate when cultured on stiffer (200 kPa) vs. softer substrates (16 kPa). In contrast, our study found that keratinocyte velocities were faster on *soft* (nominal $E = 1.2$ kPa) as opposed to *stiff* (nominal $E = 24$ kPa) PA gels. Furthermore, other researchers have observed that the proliferation/growth of fully-formed epithelial sheets *in vitro* (Madin–Darby canine kidney epithelial cells) is effectively *independent* of substrate stiffness.[36] These apparent contradictions can

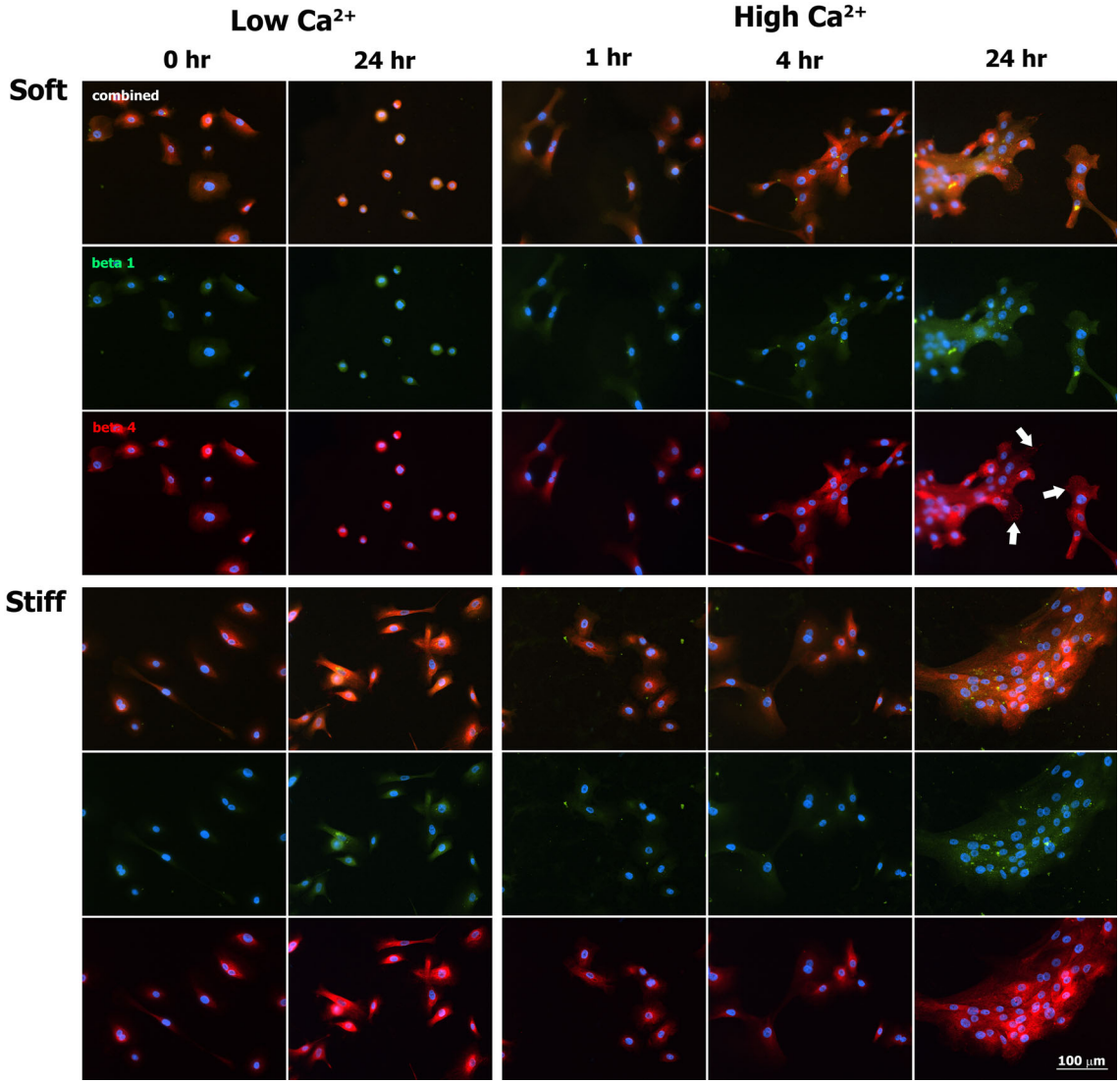

FIGURE 8. Immunofluorescence images of β4 (red), β1 (green), and nuclei (blue) in normal human epidermal keratinocytes cultured for select times on *soft* and *stiff* PA gels exposed to both *Low* Ca^{2+} and *High* Ca^{2+} conditions. White arrows indicate punctate staining of β4 on the colony periphery at 24 h in *High* Ca^{2+} conditions on soft gels.

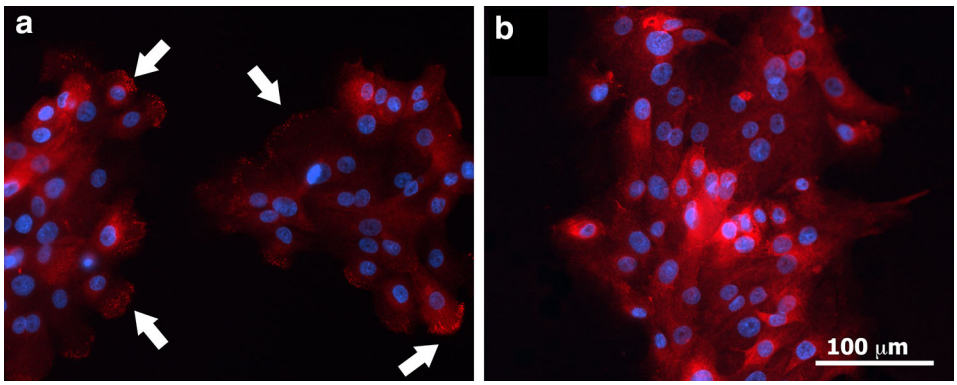

FIGURE 9. Immunofluorescence images of β4 (red) and nuclei (blue) in normal human epidermal keratinocytes cultured for 24 h in *High* Ca^{2+} conditions on (a) *soft* and (b) *stiff* PA gels. White arrows highlight areas of punctate staining observed in peripheral keratinocytes within colonies cultured on *soft* gels.

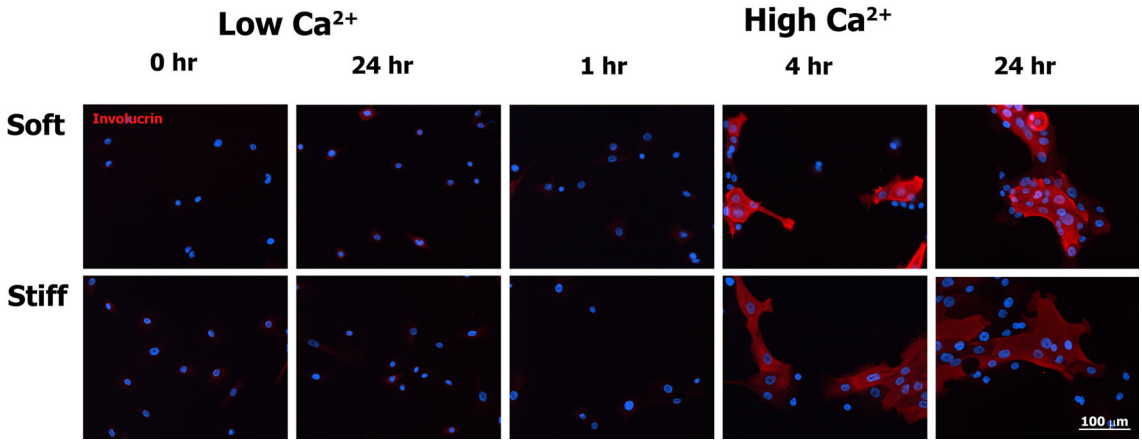

FIGURE 10. Immunofluorescence images of involucrin (red) and nuclei (blue) in normal human epidermal keratinocytes cultured for select times on *soft* and *stiff* PA gels exposed to both *Low* Ca^{2+} and *High* Ca^{2+} conditions.

possibly be explained by more careful consideration of the collective number of cell–cell and cell–matrix contacts present, in addition to consideration of the biochemical milieu the keratinocytes are exposed to at the time the observations are made, i.e., it is possible that the effect of substrate stiffness depends on whether or not one assays (i) *individual* keratinocytes during their initial attempts at colony formation (nascent epithelial sheet formation) vs. (ii) keratinocytes incorporated into a fully-developed epithelial sheet (associated with fully-formed cell–cell desmosomes and adherens junctions) vs. (iii) keratinocytes within a fully-developed but physically damaged epithelial sheet surrounded by cytokines and other paracrine signals released from adjacent damaged cells.

As gleaned from our time-lapse DIC images, the process of colony formation involves a number of dynamic and interrelated mechanobiological phenomena that make precise quantification of keratinocyte behavior difficult: individual cells, couples, and colonies are moving both towards and away from each other *via* cell–matrix tractions imposed on their underlying substrate, all the while forming transient and sometimes permanent cell–cell junctions in an attempt to form a nascent epithelial sheet. To begin to quantify some of the collective behaviors that are more qualitatively apparent to the eye of the observer, we developed two *ad hoc* analyses, termed the DR and the RC. Both DR and RC provide an indication of how close keratinocytes need to be to a forming colony in order to join that colony, and both metrics suggest that keratinocyte that keratinocytes cultured on *soft* PA gels form colonies in an increasingly *cooperative* process compared to the process of colony formation observed for keratinocytes cultured on *stiff* PA gels.

A cooperativity-like phenomenon has been qualitatively observed by other groups, specifically Guo *et al.*,[13] where they observed the spontaneous formation of tissue-like "spheroids" in both fibroblasts and NRK-52E epithelial cells cultured on soft substrates (nominal $E = 2.49$ kPa). In a similar fashion, Reinhart-King *et al.* observed that individual endothelial cell migration becomes restricted when endothelial cells are cultured in close proximity to other cells on substrates with nominal stiffness ranging between 2.5 and 5.5 kPa.[28] With their migration velocities restricted, endothelial cells exhibit increasing cell–cell contact events that may represent a nidus for tissue formation. In their work, Rheinhart-King *et al.* postulated that this form of tissue genesis may arise *via* cell–cell mechanical communication that occurs through local substrate displacements.

The results of our study are also in agreement with the idea of cell–cell mechanical signaling generated *via* local substrate displacements, specifically, the enhanced cooperativity of nascent epithelial sheet formation that we observed in keratinocytes cultured on *soft* substrates (Fig. 4). Under *High* Ca^{2+} conditions, keratinocyte colonies produced large substrate displacements, the magnitude of which increased temporally in correlation with the number of cells integrated into a given colony. Surprisingly, in comparing integrin expression between cells cultured on *soft* vs. *stiff* substrates, we found a distinct difference in the expression of the $\beta 4$ integrin subunit, specifically, the localization of $\beta 4$ to the cell–matrix interface within keratinocytes positioned along the periphery of colonies on *soft* PA gels. *In vivo*, the $\alpha 6\beta 4$ integrin (i.e., hemidesmosome) mechanically couples the keratin intermediate filament system to the basement membrane.[37] *In vitro*, true ultrastructurally complete hemidesmosomes have not been demonstrated in primary keratinocyte cultures,[37] and in our experiments, we did not perform any IF for co-staining of $\beta 4$ integrin and

keratin to see if these proteins also co-localized to the periphery of our cell colonies. However, recent work has suggested that $\alpha6\beta4$ integrin also plays a role in the regulation of keratinocyte migration *via* signaling through Rac1 to the actin-severing protein cofilin present within the lamellipodia of a motile cell.[14,30] In other words, $\alpha6\beta4$ integrins can interact (indirectly and possibly directly) with the microfilament network as opposed to being strictly confined to adynamic mechanical contacts with the keratin intermediate filament network. Thus, it is conceivable that the presence of $\beta4$ integrin in peripheral keratinocytes within colonies forming on *soft* gels is associated with the large substrate displacements generated by these colonies, though with respect to the results presented here, we can only speculate as to whether this association is one of correlation or causality.

It is important to note that presence of a *soft* substrate alone cannot account for the enhanced colony formation observed in our *High* Ca^{2+} experiments. If it did, then one might expect enhanced colony formation to occur in our *Low* Ca^{2+} control experiments, but this was not the case (Movie S1). We also considered whether the increase in calcium concentration associated with our *High* Ca^{2+} medium could in some way contribute to the differences in colony formation observed in our experiments *via* a direct effect on integrin function. Integrin binding is dependent on the presence of extracellular divalent cations, with preference for magnesium and manganese over calcium.[20] Changes in the concentration of extracellular Mg^{2+} and Ca^{2+} have been shown to differentially influence $\beta1$ integrin-associated keratinocyte adhesion and migration on type I collagen, with calcium having a mild inhibitory effect at concentrations lower than 2 mM and a more prominent inhibitory effect at calcium concentrations greater than 2 mM.[12,19] Following the calcium switch to *High* Ca^{2+} medium, it is conceivable that the formation of cadherin-mediated cell–cell contacts occurs at the expense of diminished integrin functionality, as changes in cell–cell and cell–matrix contacts are both a cause and consequence of keratinocyte differentiation. Whatever role calcium-induced changes in integrin function might play in the process of keratinocyte colony formation, the keratinocytes cultured on both our *soft* and *stiff* gels would be affected equally. Thus, the observed differences in cooperativity should be due primarily to the effect of substrate stiffness.

Incorporating *all* of our observed experimental findings, we hypothesize that the enhanced cooperativity of colony formation (nascent keratinocyte sheet formation) observed in our *soft* gel experiments arises in the following fashion. First, increased calcium concentrations in our *High* Ca^{2+} experiments enable the formation of stronger cell–cell adhesive contacts (adherens junctions and desmosomes) that maintain intercellular adhesion within an evolving colony. Second, as cell–cell tension increases within an evolving colony, cell-substrate tractions along the perimeter of the colony are increased in order to maintain mechanical equilibrium. Third, local substrate displacements- associated with the localization of $\beta4$ integrin and its direct or indirect interactions with the microfilament network- develop at the periphery of the colony in response to the increased tractions exerted by the colony. Neighboring but unattached keratinocytes then sense local deformations in the substrate and preferentially migrate towards the colony (Fig. 4, Movie S7). Thus, by means of mechanical communication through deformations in the substrate, more and more keratinocytes are recruited to join the nascent epithelial sheet in a more directed manner that occurs on a stiff substrate. Whether the keratinocytes are responding directly to gradients in substrate tension, strain, or stiffness is unclear. With regard to the latter, although PA gels are generally regarded as linear elastic materials of constant stiffness, it has been reported by Boudou *et al.* that PA gels used for cell TFM can behave as nonlinear elastic materials, exhibiting a strain-stiffening response for substrate displacements of as little as 2 to 6 μm.[4] Since the substrate displacements on the soft PA gels in *High* Ca^{2+} observed in this study were large (average of 19.4 ± 21.2 μm at $t = 24$ h), it is conceivable that the keratinocytes on soft gels demonstrated enhanced cooperativity of colony formation as a result of a the formation of stiffness gradients in the substrate rather than displacement gradients. Such a mechanism would be consistent with reports of durotaxis observed in cells cultured in nonlinear fibrous gels.[29,42]

In closing, with regards to pathophysiological relevance, note that the stiffnesses of the PA gels used in this study are consistent with atomic force microscopy (AFM) measurements of the stiffness of the human papillary dermis, specifically, 0.82 and 1.12 kPa (median elastic moduli) for specimens of papillary dermis extracted from breast and abdominal skin, respectively.[1] These measurements provide a clearer picture of the substrate stiffnesses that keratinocytes might perceive *in vivo*, and they are substantially lower than values of elastic modulus reported from macroscopic tissue-level mechanical tests.[24] Along similar lines, AFM measurements on wounded rat skin found that the elastic modulus of granulation tissue increased from 18.5 kPa at day 7 to 29.4 kPa at day 9.[11] Because the process of re-epithelialization during wound healing takes place on a bed of granulation tissue that changes its stiffness and biochemical composition as a function of time, we believe that keratinocyte colony formation (and hence

nascent epithelial sheet development) is mediated, at least in part, by durotaxis occurring at the cellular level. Furthermore, the fibrous nature of granulation tissue and ECM likely extends the potential roles of durotaxis and mechanosensing across much larger distances than is observed on non-fibrous materials of comparable stiffness, such as PA gels.[29,42] If true, building from the results of our initial experiments, one can envision new wound care therapies that target keratinocyte mechanobiology with the goal of speeding-up the rate of re-epithelialization of chronic wounds.

CONCLUSION

As observed in our experiments, keratinocytes cultured on pepsin digested type I collagen coated *soft* PA gels exhibit (i) smaller spread contact areas, (ii) increased migration velocities, and (iii) increased rates of colony formation with more cells per colony than do keratinocytes cultured on *stiff* gels. Together with the differences observed in substrate displacements, DR, and RC, our findings are reflective of what we perceive as increasingly *cooperative* behavior of keratinocytes cultured on *soft* vs. *stiff* gels during the process of colony formation, i.e., the observation that individual cells, couples, and colonies cultured on *soft* gels under *High* Ca^{2+} conditions seem to better coordinate their efforts to achieve local nascent epithelial sheet formation compared to the increasingly stochastic cell–cell contact events that lead to nascent sheet formation from similar collections of cells, couples, and colonies cultured on *stiff* substrates. Although more work is required to elucidate the specific mechanobiological mechanisms involved, we hypothesize that the differences in keratinocyte colony formation observed in our experiments are associated with an enhanced expression of β4 integrin along the periphery of colonies evolving on *soft* substrates which ultimately lead to increased cell–cell mechanical signaling generated *via* local substrate deformations.

ELECTRONIC SUPPLEMENTARY MATERIAL

The online version of this article (doi:10.1007/s12195-015-0377-8) contains supplementary material, which is available to authorized users.

ACKNOWLEDGEMENTS

Support for this project was provided by the National Institutes of Health (R03-AR063967) and the Roy J. Carver Charitable Trust (#14-4384). We thank Kelly Messingham for assistance with immunolabeling, and Janet Fairley, George Giudice, and Thomas Magin for insightful discussions on this work.

CONFLICT OF INTEREST

Hoda Zarkoob, Sandeep Bodduluri, Sailahari V. Ponnaluri, John C. Selby, and Edward A. Sander declare that they have no conflict of interest.

ETHICAL STANDARDS

No human or animal studies or were carried out by the authors for this article.

REFERENCES

[1]Achterberg, V. F., L. Buscemi, H. Diekmann, J. Smith-Clerc, H. Schwengler, J. J. Meister, *et al*. The nano-scale mechanical properties of the extracellular matrix regulate dermal fibroblast function. *J. Invest. Dermatol.* 134(7):1862–1872, 2014.

[2]Anon, E., X. Serra-Picamal, P. Hersen, N. C. Gauthier, M. P. Sheetz, X. Trepat, *et al*. Cell crawling mediates collective cell migration to close undamaged epithelial gaps. *Proc. Natl. Acad. Sci. USA* 109(27):10891–10896, 2012.

[3]Aratyn-Schaus, Y., P. W. Oakes, J. Stricker, S. P. Winter, and M. L. Gardel. Preparation of complaint matrices for quantifying cellular contraction. *J. Visualized Exp.* 46:2170, 2010.

[4]Boudou, T., J. Ohayon, C. Picart, R. I. Pettigrew, and P. Tracqui. Nonlinear elastic properties of polyacrylamide gels: implications for quantification of cellular forces. *Biorheology* 46(3):191–205, 2009.

[5]Butler, J. P., I. M. Tolic-Norrelykke, B. Fabry, and J. J. Fredberg. Traction fields, moments, and strain energy that cells exert on their surroundings. *Am. J. Physiol. Cell Physiol.* 282(3):C595–C605, 2002.

[6]Chan, S. H., D. T. Võ, and T. Q. Nguyen, (ed.). Subpixel Motion Estimation Without Interpolation. IEEE International Conference on Acoustics Speech and Signal Processing (ICASSP), IEEE, 2010.

[7]Cras, J., C. Rowe-Taitt, D. Nivens, and F. Ligler. Comparison of chemical cleaning methods of glass in preparation for silanization. *Biosensors Bioelectron.* 14(8):683–688, 1999.

[8]Doyle, A. D., F. W. Wang, K. Matsumoto, and K. M. Yamada. One-dimensional topography underlies three-dimensional fibrillar cell migration. *J. Cell Biol.* 184(4):481–490, 2009.

[9]Eming, S. A. Biology of Wound Healing. In: Dermatology, edited by J. L. Bolognia, J. L. Jorizzo, and J. V. Schaffer. Philadephia: Elsevier Saunders, 2012.

[10]Evans, N. D., R. O. Oreffo, E. Healy, P. J. Thurner, and Y. H. Man. Epithelial mechanobiology, skin wound healing, and the stem cell niche. *J. Mech. Behav. Biomed. Mater.* 28:397–409, 2013.

[11]Goffin, J. M., P. Pittet, G. Csucs, J. W. Lussi, J. J. Meister, and B. Hinz. Focal adhesion size controls tension-depen-

dent recruitment of alpha-smooth muscle actin to stress fibers. *J. Cell. Biol.* 172(2):259–268, 2006.
[12]Grzesiak, J. J., and M. D. Pierschbacher. Changes in the concentrations of extracellular Mg^{++} and Ca^{++} down-regulate E-cadherin and up-regulate alpha 2 beta 1 integrin function, activating keratinocyte migration on type I collagen. *J. Invest. Dermatol.* 104(5):768–774, 1995.
[13]Guo, W. H., M. T. Frey, N. A. Burnham, and Y. L. Wang. Substrate rigidity regulates the formation and maintenance of tissues. *Biophys. J.* 90(6):2213–2220, 2006.
[14]Hamill, K. J., S. B. Hopkinson, P. DeBiase, and J. C. Jones. BPAG1e maintains keratinocyte polarity through beta4 integrin-mediated modulation of Rac1 and cofilin activities. *Mol. Biol Cell* 20(12):2954–2962, 2009.
[15]Hartwig, B., B. Borm, H. Schneider, M. J. Arin, G. Kirfel, and V. Herzog. Laminin-5-deficient human keratinocytes: defective adhesion results in a saltatory and inefficient mode of migration. *Exp. Cell Res.* 313(8):1575–1587, 2007.
[16]Hunyadi, J., B. Farkas, C. Bertenyi, J. Olah, and A. Dobozy. Keratinocyte grafting: a new means of transplantation for full-thickness wounds. *J. Dermatol. Surg. Oncol.* 14(1):75–78, 1988.
[17]Kim, J. H., X. Serra-Picamal, D. T. Tambe, E. H. Zhou, C. Y. Park, M. Sadati, *et al.* Propulsion and navigation within the advancing monolayer sheet. *Nat. Mater.* 12(9):856–863, 2013.
[18]Kirsner, R. S., W. A. Marston, R. J. Snyder, T. D. Lee, D. I. Cargill, and H. B. Slade. Spray-applied cell therapy with human allogeneic fibroblasts and keratinocytes for the treatment of chronic venous leg ulcers: a phase 2, multicentre, double-blind, randomised, placebo-controlled trial. *Lancet* 380(9846):977–985, 2012.
[19]Lange, T. S., A. K. Bielinsky, K. Kirchberg, I. Bank, K. Herrmann, T. Krieg, *et al.* Mg^{2+} and Ca^{2+} differentially regulate beta 1 integrin-mediated adhesion of dermal fibroblasts and keratinocytes to various extracellular matrix proteins. *Exp. Cell Res.* 214(1):381–388, 1994.
[20]Lange, T. S., J. Kirchberg, A. K. Bielinsky, A. Leuker, I. Bank, T. Ruzicka, *et al.* Divalent cations (Mg^{2+}, Ca^{2+}) differentially influence the beta 1 integrin-mediated migration of human fibroblasts and keratinocytes to different extracellular matrix proteins. *Exp. Dermatol.* 4(3):130–137, 1995.
[21]Leigh, I. M., and F. M. Watt. The Culture of Human Epidermal Keratinocytes. The Keratinocyte Handbook. Cambridge: Cambridge University Press, pp. 43–51, 1994.
[22]Martin, P. Wound healing-aiming for perfect skin regeneration. *Science* 276(5309):75–81, 1997.
[23]Mertz, A. F., Y. Che, S. Banerjee, J. M. Goldstein, K. A. Rosowski, S. F. Revilla, *et al.* Cadherin-based intercellular adhesions organize epithelial cell–matrix traction forces. *Proc. Natl. Acad. Sci. USA* 110(3):842–847, 2013.
[24]NiAnnaidh, A., K. Bruyere, M. Destrade, M. D. Gilchrist, and M. Ottenio. Characterization of the anisotropic mechanical properties of excised human skin. *J. Mech. Behav. Biomed. Mater.* 5(1):139–148, 2012.
[25]Pelham, Jr, R. J., and Y. Wang. Cell locomotion and focal adhesions are regulated by substrate flexibility. *Proc. Natl. Acad. Sci. USA* 94(25):13661–13665, 1997.
[26]Peyton, S. R., and A. J. Putnam. Extracellular matrix rigidity governs smooth muscle cell motility in a biphasic fashion. *J. Cell. Physiol.* 204(1):198–209, 2005.
[27]Raghupathy, R., C. Witzenburg, S. P. Lake, E. A. Sander, and V. H. Barocas. Identification of regional mechanical anisotropy in soft tissue analogs. *J. Biomech. Eng.* 133(9):091011, 2011.
[28]Reinhart-King, C. A., M. Dembo, and D. A. Hammer. Cell–cell mechanical communication through compliant substrates. *Biophys. J.* 95(12):6044–6051, 2008.
[29]Rudnicki, M. S., H. A. Cirka, M. Aghvami, E. A. Sander, Q. Wen, and K. L. Billiar. Nonlinear strain stiffening is not sufficient to explain how far cells can feel on fibrous protein gels. *Biophys. J.* 105(1):11–20, 2013.
[30]Sehgal, B. U., P. J. DeBiase, S. Matzno, T. L. Chew, J. N. Claiborne, S. B. Hopkinson, *et al.* Integrin beta4 regulates migratory behavior of keratinocytes by determining laminin-332 organization. *J. Biol. Chem.* 281(46):35487–35498, 2006.
[31]Selby, J. C. Mechanobiology of Epidermal Keratinocytes: Desmosomes, Hemidesmosomes, Keratin Intermediate Filaments, and Blistering Skin Diseases. Mechanobiology of Cell–Cell and Cell–Matrix Interactions. Berlin: Springer, pp. 169–210, 2011.
[32]Selby, J. C., and M. A. Shannon. Mechanical response of a living human epidermal keratinocyte sheet as measured in a composite diaphragm inflation experiment. *Biorheology* 44(5–6):319–348, 2007.
[33]Tang, X., A. Tofangchi, S. V. Anand, and T. A. Saif. A novel cell traction force microscopy to study multi-cellular system. *PLoS Comput. Biol.* 10(6):e1003631, 2014.
[34]Toyjanova, J., E. Bar-Kochba, C. Lopez-Fagundo, J. Reichner, D. Hoffman-Kim, and C. Franck. High resolution, large deformation 3D traction force microscopy. *PloS ONE* 9(4):e90976, 2014.
[35]Trappmann, B., J. E. Gautrot, J. T. Connelly, D. G. Strange, Y. Li, M. L. Oyen, *et al.* Extracellular-matrix tethering regulates stem-cell fate. *Nat. Mater.* 11(7):642–649, 2012.
[36]Trepat, X., M. R. Wasserman, T. E. Angelini, E. Millet, D. A. Weitz, J. P. Butler, *et al.* Physical forces during collective cell migration. *Nat. Phys.* 5(6):426–430, 2009.
[37]Tsuruta, D., T. Hashimoto, K. J. Hamill, and J. C. Jones. Hemidesmosomes and focal contact proteins: functions and cross-talk in keratinocytes, bullous diseases and wound healing. *J. Dermatol. Sci.* 62(1):1–7, 2011.
[38]Wang, Y., G. Wang, X. Luo, J. Qiu, and C. Tang. Substrate stiffness regulates the proliferation, migration, and differentiation of epidermal cells. *Burns* 38(3):414–420, 2012.
[39]Watt, F. M. Influence of cell shape and adhesiveness on stratification and terminal differentiation of human keratinocytes in culture. *J. Sci. Suppl.* 8:313–326, 1987.
[40]Watt, F. M., P. W. Jordan, and C. H. O'Neill. Cell shape controls terminal differentiation of human epidermal keratinocytes. *Proc. Natl. Acad. Sci. USA* 85(15):5576–5580, 1988.
[41]Wen, J. H., L. G. Vincent, A. Fuhrmann, Y. S. Choi, K. C. Hribar, H. Taylor-Weiner, *et al.* Interplay of matrix stiffness and protein tethering in stem cell differentiation. *Nat. Mater.* 13(10):979–987, 2014.
[42]Winer, J. P., S. Oake, and P. A. Janmey. Non-linear elasticity of extracellular matrices enables contractile cells to communicate local position and orientation. *PloS ONE* 4(7):e6382, 2009.
[43]Zamansky, G. B., U. Nguyen, and I. N. Chou. An immunofluorescence study of the calcium-induced coordinated reorganization of microfilaments, keratin intermediate filaments, and microtubules in cultured human epidermal keratinocytes. *J. Invest. Dermatol.* 97(6):985–994, 1991.